New evidence from seismic imaging for subduction during assembly of the North China craton

Tianyu Zheng*, Liang Zhao, and Rixiang Zhu
Seismological Laboratory (SKL-LE), Institute of Geology and Geophysics, Chinese Academy of Sciences, Beijing 100029, China

ABSTRACT

The "frozen-in" information in the crust plays an important role in improving our understanding of cratonic formation and evolution and plate tectonics in the Precambrian. The Trans-North China orogen is a continent-continent collision belt generated by the assembly of the North China craton. The mechanism and modality of the collision are disputed. Here we present a seismic image of the Western block and the Trans-North China orogen of the North China craton derived using receiver function analysis of the teleseismic records from a dense array. A low-velocity zone extending from the middle crust to the Moho is interpreted as a remnant of upper-middle crustal material associated with westward-dipping subduction beneath the Western block of the North China craton. Crustal uplift and magmatic underplating resulting from subsequent tectonic events were responsible for modifying the remaining subduction architecture. The western boundary of the Trans-North China orogen is located west of the boundary earlier identified by surface investigation. The results, combined with previous seismic imaging in the eastern North China craton, provide insight into the amalgamation of the Eastern and Western blocks and the subsequent tectonic deformation of the North China craton.

INTRODUCTION

The style of the plate tectonics of the Proterozoic and Archean Earth is disputed. However, some Precambrian orogenic belts did not undergo postcollisional deformation or magmatism, and therefore can yield clues about the time of initiation and the style of tectonics. The first discovery of a subduction-related structure indicating Paleoproterozoic plate tectonics was a fossil mantle suture in the Svecofennian orogen (1.89 Ga) of the Baltic shield, detected using seismic reflection imaging (BABEL Working Group, 1990). Further evidence came from reflection images of the Paleoproterozoic and Neoarchean collision zones in Canada, including the Trans-Hudson orogen, the Wopmay orogen, and the amalgamation belts in the Superior Province. The imaging suggested that dipping crustal reflectors, which extended from the lower crust into the upper mantle, were a relic of plate convergence, subduction, and accretion (Calvert et al., 1995; Cook et al., 1999; White et al., 2000). As one of the oldest continent blocks in the proposed Paleoproterozoic–Mesoproterozoic supercontinent (Wilde et al., 2002), the North China craton is a promising region for study that may provide evidence of early global plate movements.

To understand the tectonic processes involved in the assembly of the North China craton, a dense seismic array of 50 temporary stations (numbered 258–308, excluding 261) from a sub-project of the North China Interior Structure Project (NCISP-4) was operated from September 2005 to September 2006. The average spacing was ~10 km. The thick Quaternary sedimentary cover of the central part of the Ordos basin is unsuitable for seismic observations, so we deployed the stations at the northern edge of the Ordos (see profile A–B in Fig. 1). A seismic profile crossing the Eastern and Western blocks along an east-west transect was constructed by combining the NCISP-4 with the NCISP-2 array. The published results from NCISP-2 (Zheng et al., 2006) were combined in this study.

GEOLOGIC SETTING

The North China craton is one of the world's oldest, preserving continental rocks as old as 3.8 Ga; the basement consists of variably exposed Archean–Paleoproterozoic rocks (Zhao et al., 2001). Mesoproterozoic unmetamorphosed volcanic-sedimentary successions and Phanerozoic cover unconformably overlie the basement. The basement of the North China craton can be divided into the Eastern and Western blocks (Fig. 1), which developed independently during the Archean (Zhao et al., 2001).

The Western block can be further subdivided into the Ordos block in the south and the Yinshan block in the north; the east-west–trending Khondalite belt is between the two blocks. At 1.92 Ga, the southern margin of the Yinshan block was amalgamated to the northern margin of the Ordos block, leading to high-grade metamorphism of the Khondalite belt (Santosh et al., 2007).

In the Late Archean to early Paleoproterozoic, subduction beneath the Eastern block led to the formation of island and magmatic arcs that were subsequently incorporated into the central zone. Continued subduction resulted in a major continent-continent collision between the Eastern and Western blocks and the final amalgamation of the North China craton ca. 1.85 Ga, forming the north-south–trending collisional orogen, named the Trans-North China orogen (Zhao et al., 2005).

The well-exposed Wutaishan-Hengshan-Fuping-Lüliangshan terranes constitute a representative transect across the Trans-North China orogen that delimits the Late Archean–Paleoproterozoic accretion and assembly of the North China craton (Faure et al., 2007). This Precambrian terrane was uplifted in the Mesozoic and Cenozoic, as indicated by dome shapes, and is considered by many to be tectonically coupled with the sinking of the Bohai Bay basin in the Eastern block. Previous investigations have revealed a contrasting thickness and composition of the lithospheric mantle beneath the eastern North China craton between the Paleozoic and present time, indicating its reactivation in the Mesozoic (Menzies et al., 1993; Griffin et al., 1998).

SEISMIC IMAGING

In this study, radial receiver functions from 49 of the 50 stations of the NCISP-4 (A–B profile in Fig. 1) (data from station 264 were not used because of strong site noise) and three stations (197, 199, and 200) of the NCISP-2 (B–C profile in Fig. 1) were used to image the structures of the crustal and upper mantle beneath the observation profile. For brevity, this profile, crossing the Western block to the Trans-North China orogen, is termed WTP. The data set contains 3183 receiver functions, which were then stacked for each station (Fig. 2A). The Ps phases from the Moho (~5–6 s) were clearly observed at all stations. Strong waveform variations were observed in the stacked receiver function section, indicating the presence of strong structural heterogeneities beneath the study region.

An integrated receiver function imaging technique (Zheng et al., 2006) was used, which involves iteratively implementing waveform inversion and common conversion point (CCP) stacking of receiver functions. This technique permits exploration of detailed crustal features. During the process, a CCP imaging method was used to identify the major velocity discontinuities in the crust, while a waveform inversion technique was performed to reconstruct a velocity structure. Figure 2B shows the derived synthetic receiver functions, which are in good agreement with the records shown in Figure 2A with respect to both waveform and relative

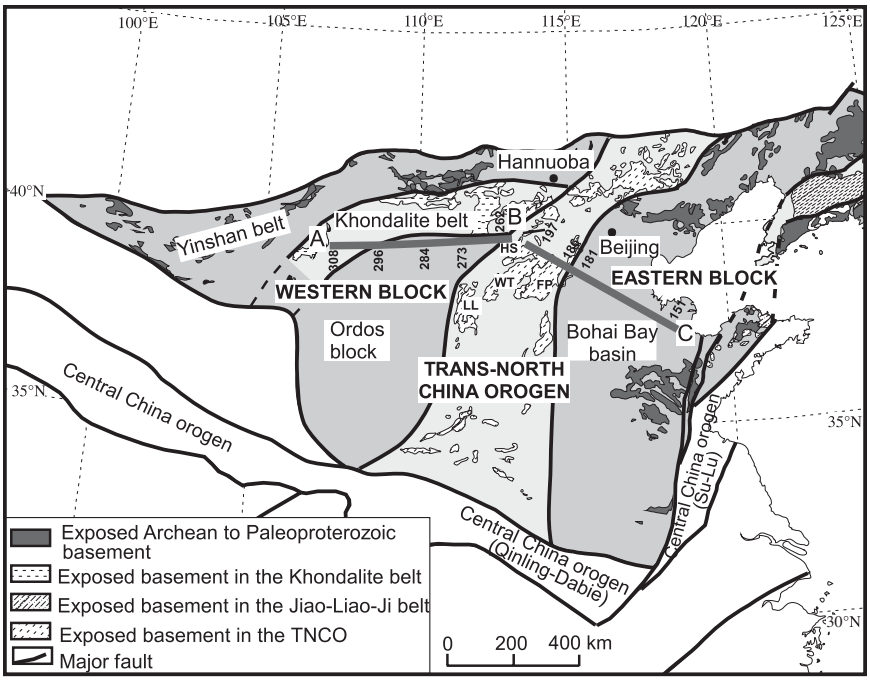

Figure 1. Simplified tectonic map of North China craton showing exposed basement and major tectonic units, including the Eastern block, the Western block, and the Trans-North China orogen (TNCO) (modified from Zhao et al., 2005). Thick solid lines represent seismic observation profiles AB (NCISP-4) and BC (NCISP-2), with some selected station numbers marked alongside. FP—Fuping, HS—Hengshan, LL—Lüliang, WT—Wutai.

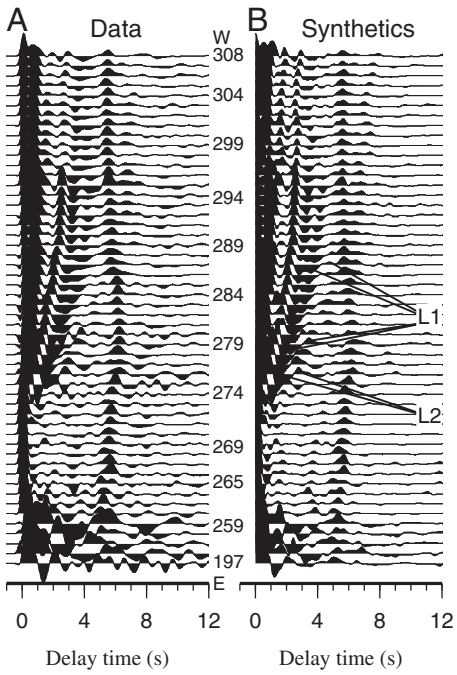

Figure 2. Cross sections (from east to west) of P-receiver functions. A: Data from stacking. B: Synthetics. Traces are plotted in a time window between −1 and 12 s with time-zero aligning with onset of the P wave. Amplitudes of traces are normalized by maximum amplitude of all the traces. Selected station numbers are labeled in A for ease of reference. Marked P-to-S phases are converted from the upper and bottom interfaces of zones L1 and L2, which are plotted in Figure 3.

amplitude (see the GSA Data Repository[1] for more details about the data processing, imaging method, results, and the reliability analysis).

The CCP image of the WTP shows three significant features (Fig. 3A): (1) distinct crustal structures characterized by undulate interfaces in the east and flat-lying interfaces in the west; (2) strong negative Ps polarities (marked by the brown color traces with superposed blue points in Fig. 3A), reflecting a reversal from high to low velocities with increase in depth; and (3) westward-dipping interfaces of a low-velocity zone (L1) from the upper crust to the Moho beneath stations 274–296.

The optimal shear-wave velocity image of the WTP (beneath stations 197–308) was compiled from the inverted velocity model (Fig. 3B). For a large-scale view, we also present the available crustal velocity image to the east (beneath stations 151–196), which was discussed by Zheng et al. (2006), to delineate the crustal structure from the Bohai Bay basin in the east westward across the Trans-North China orogen and the Western block of the North China craton. Along the WTP, the data suggest a three-layer crustal structure consisting of an upper, middle, and lower crust, covered by a sedimentary sequence, with shear-wave velocities of 3.50–3.55 km/s, 3.65–3.75 km/s, and 3.80–3.90 km/s, respectively, for the crustal components. Beneath stations 297–308, the crust thickness is ~40 km, with a flat Moho and crustal layers, whereas the Moho thickens to a depth of 46 km beneath stations 275–284, forming a crustal root zone.

The WTP image exhibits the intriguing characteristic of two low-velocity zones, L1 and L2, in the crust of the Western block and the Trans-North China orogen. The polarity of the velocity change crossing the interface can be confirmed by the polarity of the conversion phase in the receiver function imaging: the low-velocity structures of L1 and L2 were diagnosed by a negative polarity of the upper-interface phase and a positive polarity of the lower-interface phase, as shown in Figure 3A. The seismic structure derived by waveform inversions shows that beneath stations 274–296, the low-velocity zone L1 (with shear velocity 3.6–3.7 km/s) extends from the bottom of the upper crust to the Moho (Fig. 3B); to the east of station 280, the relatively flat, low-velocity zone L2 (with shear velocity 3.7 km/s) is within the lower crust (Fig. 3B).

DISCUSSION AND CONCLUSIONS

As shown in the integrated image transect in Figure 3B, the diversity of the crustal structure is consistent with a threefold division of the North China craton crust. The undulating and complex structural features of the Eastern block and the Trans-North China orogen imply that these parts underwent compound tectonism after craton assembly. In the Eastern block, the thick sediments, shallow Moho, and thinned crustal fabrics support extensional tectonism and reflect the effects of the reactivation of the North China craton during the Mesozoic and Cenozoic. The undulating and dipping interfaces beneath the Trans-North China orogen are likely the consequence of both Paleoproterozoic amalgamation and subsequent uplift events. In the west (beneath stations 274–308), in contrast, the flat crustal fabrics define a stable cratonic regime.

Because the crust of the Western block has been stable over the long term with respect to temperature and pressure after the 1.8 Ga amalgamation, the velocity differences between low-velocity zones (L1 and L2) and their ambient units are mainly attributable to compositional differences and not temperature variation. The velocities (3.6–3.7 km/s) of L1 and L2 are lower than the typical lower crust values of 3.8–3.9 km/s. This may indicate a composition more akin to the upper-middle crust (mainly felsic gneiss), and implies that zone L1 may be a

[1]GSA Data Repository item 2009100, seismic observation, receiver function imaging, and reliability analysis, is available online at www.geosociety.org/pubs/ft2009.htm, or on request from editing@geosociety.org or Documents Secretary, GSA, P.O. Box 9140, Boulder, CO 80301, USA.

westward-dipping upper-middle crust remnant, and that zone L2 is an upper-middle crust remnant stagnating in the lower crust.

Several possible models can be used to interpret the L1 zone. One model is crustal overthrusting, as found, for example, in the Kapuskasing structure of the Superior craton, Canada (Boland et al., 1988). An alternative model is that crustal thickening is associated with a small block trapped during continent-continent collision, exemplified in the Trans-Hudson orogen in Canada (Lewry et al., 1994). Yet another model is a downward-dipping subducted slab that is attached to the lower crust and descends into the upper mantle, as is the case in the Svecofennian orogen and the Superior Province, Canada (BABEL Working Group, 1990; Calvert et al., 1995).

In the first scenario, crustal overthrusting, the rocks in the hanging wall should have an associated high seismic velocity rather than the low-velocity zone of L1. Based on this assumption, L1 is unlikely to have been generated by overthrusting. Regarding the second possible model, block trapped, it is difficult to interpret L1 in a similar way to the collisional sedimentary and plutonic rocks of the Trans-Hudson orogen because such weak rocks could hardly have extended to ~100 km above the Moho as the L1 low-velocity section does.

We favor that the L1 represents a remnant of upper-middle crust associated with westward subduction beneath the Western block during the assembly of the North China craton. Beneath stations 186–192, a fragmented, low-velocity zone tilts upward, representing a topography similar to that of the L1, and is possibly associated with the amalgamation of the Eastern block and the Trans-North China orogen on the east side (Fig. 3C). Faure et al. (2007) proposed a dynamic model in which the amalgamation of the North China craton took place through two stages of continental collisions, occurring at 2.1 Ga and 1.9 Ga. These two westward-dipping, low-velocity zones may be in good agreement with such a dynamic process. We speculate that the low-velocity zone L2 is possibly a slab-like remnant attached to the bottom of the original lower crust during the last stage of this subduction.

Nevertheless, there are some differences in the fossil slab configuration between L1 and the slab structures obtained from the previous seismic images (Calvert et al., 1995; Bohnhoff et al., 2001). One reason may be that conditions were different in ancient and modern subduction zones, combined with the effects of subsequent tectonism after assembly of the North China craton. Different conditions in the early Earth could have led to different processes of subduction in the Precambrian from those in the Phanerozoic. For example, higher mantle temperatures probably led to high degrees of melting

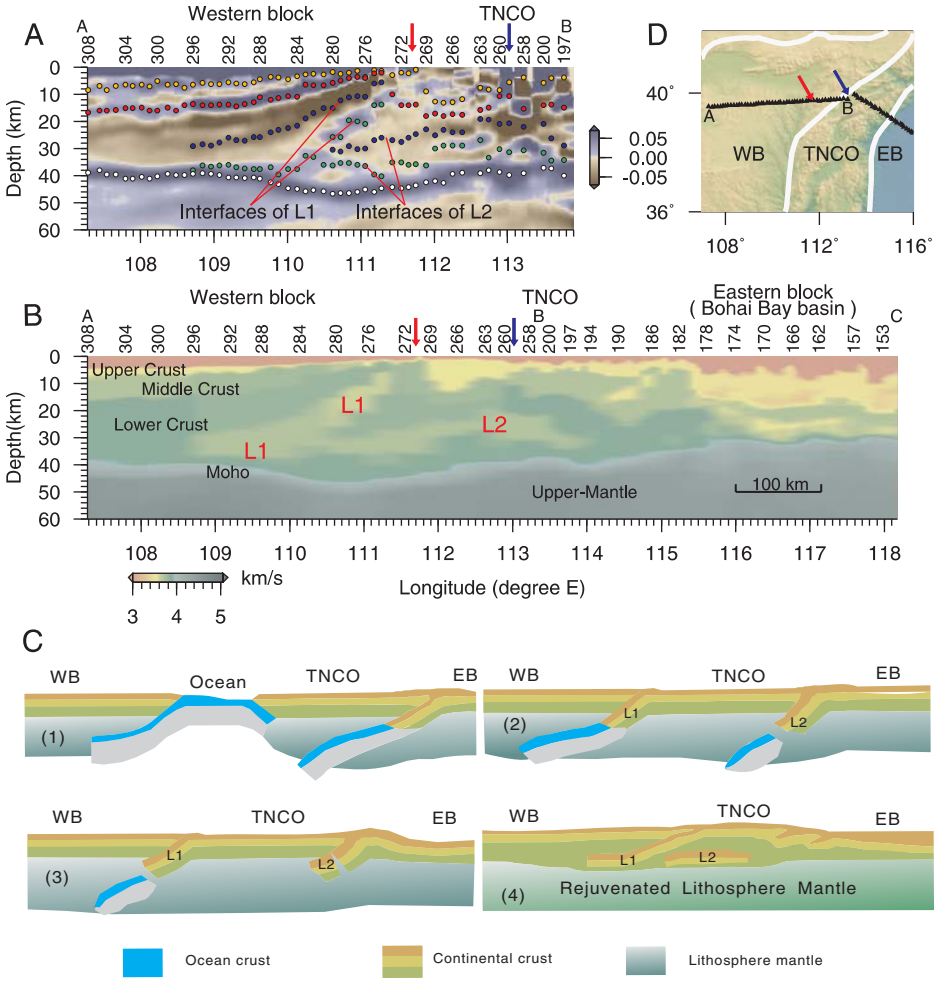

Figure 3. A: Common conversion point (CCP) receiver function image of crust and uppermost mantle along Western block–Trans-North China orogen profile (TNCO) based on the inverted velocity model. Blue represents positive (brown represents negative) amplitude of receiver function annotated in the right color bar, indicating velocity increase (or decrease) downward. Intracrustal interfaces and Moho identified in CCP image are compared with those derived from the best-fitting models by waveform inversion (Fig. DR2). Dots in CCP image mark velocity discontinuities in the best-fitting models, including upper-middle (orange) and middle-lower (red) crustal interfaces, Moho (white), the interfaces with negative velocity gradient above L1 and L2 layers (blue), and the bottom interfaces of L1 and L2 (green). B: Shear-wave velocity structure of crust and uppermost mantle compiled from inverted velocity model along east-west profile (A–B in Fig. 1 in this study, and B–C from the results of Zheng et al., 2006). L1 is a westward-dipping low-velocity zone beneath stations 274–296 that separates TNCO and Western block, and L2 is a horizontal low-velocity zone in the lower crust beneath TNCO and the Western block. C: Schematic diagram of ancient subduction model (see text for details). D: Topographic map of the study region and locations of stations. Triangles represent broadband seismic stations used in this study. Selected station numbers are labeled on top of plots in A and B. In A, B, and D, red arrow marks boundary location between Western block and TNCO identified by this study, and blue arrow marks boundary previously envisaged by Zhao et al. (2001). EB—Eastern block, WB—Western block.

at mid-oceanic ridges, which, in turn, resulted in thicker oceanic crust and perhaps flatter-dipping subduction zones (Foley et al., 2003; Smithies et al., 2003). Combining the idea of shallow subduction with the two-step evolution model of the Trans-North China orogen and the subsequent tectonic reactivation of the North China craton, we have constructed a tectonic model to interpret the imaged crustal structure (Fig. 3B), as shown in Figure 3C.

In Figure 3C, panel 1 represents the subduction of oceanic lithosphere and the drag of continental lithosphere, in which the eastern part subducted earlier than the western part. The ancient ocean crust is thicker and warmer than modern ocean crust, which resulted in a flat subduction of oceanic lithosphere. Break-off of the subducted oceanic lithosphere occurred due to the resistance to buoyancy of the continent (see panel 2 and 3 in Fig. 3C). Following

the extensional effects of slab break-off and tectonic uplifting, the continental crust dragged into the topmost upper mantle was exhumed (panel 4 in Fig. 3C), which resulted in Paleoproterozoic crustal contamination by subduction and collision between the Eastern and Western blocks (Wu et al., 2005).

After the assembly of the North China craton, the continental lithosphere was possibly modified by subsequent tectonism. Three uplift events may have occurred after assembly of the North China craton: (1) uplift prior to a 1.85–1.7Ga rift event (Zhai et al., 2005); (2) coherent uplift associated with double-convergence subduction beneath the north and south margins of the craton in the late Paleozoic to early Mesozoic; and (3) uplift of the Eastern block during the Late Jurassic and Early Cretaceous (Menzies et al., 1993). Although the precise details are unknown, it appears likely that subsequent uplift could have modified the crustal structure, with it becoming markedly shallower to the east and resulting in the L1 zone being close to the bottom of the upper crust, as shown in the WTP image (Fig. 3A). Crustal underplating that occurred in the Hannuoba area (Fig. 1) in Late Jurassic–Early Cretaceous time was been identified by petrological studies (Chen et al., 2001). The remaining oceanic and/or continental crust in the mantle was then modified during the rejuvenation process of mantle, inhibiting identification of the mantle part of the subducted lithosphere (panel 4 in Fig. 3C). The tectonic interpretation (Fig. 3C) for the imaged crustal structure (Fig. 3B) provides an understanding of the distinctive and unique features of ancient subduction.

Based on the tectonic interpretation for the WTP image, we conclude that the projection of the L1 zone to the surface (stations 270–273) (red arrow in Fig. 3D) is the boundary between the Western block and the Trans-North China orogen. The shear wave splitting results also support this view (Zhao et al., 2008). It is not surprising that the boundary is located farther west than previously thought (blue arrow in Fig. 3D) because the previous identification was mainly based on the younger faults (Zhao et al., 2001). Poor exposure of Precambrian rocks at the boundary area (stations 263–273), however, might have confused the previous interpretation.

The distinctive features of the crustal structure of the Eastern block (Bohai Bay basin), the Trans-North China orogen, and the Western block, as well as the inferred boundary structures, provide insight into the assembly and subsequent tectonic deformation of the North China craton. In summary, we propose that westward-dipping subduction is a more rational explanation for the North China craton assembly, although other possibilities are not precluded. The surface location of the western boundary of the Trans-North China orogen is sited west of the previously identified surface location (Zhao et al., 2001). Subsequent tectonic activity, including crustal uplift and underplating, may have modified the subduction architecture.

ACKNOWLEDGEMENTS

We gratefully acknowledge the researchers at the Seismic Array Laboratory, Institute of Geology and Geophysics, Chinese Academy of Sciences. We thank S.A. Wilde for his constructive comments, and W.P. Schellart and anonymous reviewers for valuable comments and constructive suggestions. This work was supported by the National Natural Science Foundation of China (40434012) and the Chinese Academy of Sciences.

REFERENCES CITED

BABEL Working Group, 1990, Evidence for early Proterozoic plate tectonics from seismic reflection profiles in the Baltic shield: Nature, v. 348, p. 34–38, doi: 10.1038/348034a0.

Bohnhoff, M., Makris, J., Papanikolaou, D., and Stavrakaki, G., 2001, Crustal investigation of the Hellenic subduction zone using wide aperture seismic data: Tectonophysics, v. 343, p. 239–262, doi: 10.1016/S0040-1951(01)00264-5.

Boland, A.V., Ellis, R.M., Northey, D.J., West, G.F., Green, A.G., Forsyth, D.A., Mereu, R.F., Meyer, R.F., Morel-à-ihuissier, P., Buchbinder, G.G.R., Asudeh, I., and Haddon, R.A.W., 1988, Seismic delineation of upthrust Archaean crust in Kapuskasing, northern Ontario: Nature v. 335, p. 711–713.

Calvert, A.J., Sawyer, E.W., Davis, W.J., and Ludden, J.N., 1995, Archaean subduction inferred from seismic images of a mantle suture in the Superior Province: Nature, v. 375, p. 670–674, doi: 10.1038/375670a0.

Chen, S.H., O'Reilly, S.Y., Zhou, X.H., Griffin, W.L., Zhang, G.W., Sun, M., Feng, J.L., and Zhang, M., 2001, Thermal and petrological structure of the lithosphere beneath Hannuoba, Sino-Korean Craton, China: Evidence from xenoliths: Lithos, v. 56, p. 267–301, doi: 10.1016/S0024-4937(00)00065-7.

Cook, F.A., van der Velden, A.J., Hall, K.W., and Roberts, B.J., 1999, Frozen subduction in Canada's Northwest Territories: Lithoprobe deep seismic reflection profiling of the western Canadian shield: Tectonics, v. 18, p. 1–24, doi: 10.1029/1998TC900016.

Faure, M., Trapp, P., Lin, W., Monié, P., and Bruguier, O., 2007, Polyorogenic evolution of the Paleoproterozoic Trans-North China Belt—New insights from the Lüliangshan-Hengshan-Wutaishan and Fuping massifs: Episodes, v. 30, p. 95–106.

Foley, S.F., Buhre, S., and Jacob, D.E., 2003, Evolution of the Archean crust by delamination and shallow subduction: Nature, v. 421, p. 249–252, doi: 10.1038/nature01319.

Griffin, W.L., Zhang, A., O'Reilly, S.Y., and Ryan, C.D., 1998, Phanerozoic evolution of the lithosphere beneath the Sino-Korean craton, *in* Flower, M.F.J., et al., eds., Dynamics and plate interactions in East Asia: American Geophysical Union Geodynamics Series 27, p. 107–126.

Lewry, J.F., Hajnal, Z., Green, A., Lucas, S.B., White, D., Stauffer, M.R., Ashton, K.E., Weber, W., and Clowes, R., 1994, Structure of a Paleoproterozoic continent-continent collision zone: A Lithoprobe seismic reflection profile across the Trans-Hudson orogen, Canada: Tectonophysics, v. 232, p. 143–160, doi: 10.1016/0040-1951(94)90081-7.

Menzies, M.A., Fan, W.M., and Zhang, M., 1993, Palaeozoic and Cenozoic lithoprobes and the loss of >120 km of Archaean lithosphere, Sino-Korean craton, China, *in* Prichard, H.M., et al., eds., Magmatic processes and plate tectonics: Geological Society of London Special Publication 76, p. 71–81.

Santosh, M., Wilde, S.A., and Li, J.H., 2007, Timing of Paleoproterozoic ultrahigh-temperature metamorphism in the North China Craton: Evidence from SHRIMP U-Pb zircon geochronology: Precambrian Research, v. 159, p. 178–196, doi: 10.1016//j.precamres.2007.06.006.

Smithies, R.H., Champion, D.C., and Cassidy, K.F., 2003, Formation of Earth's early Archaean continental crust: Precambrian Research, v. 127, p. 89–101, doi: 10.1016/S0301-9268(03)00182-7.

White, D.J., Zwanzig, H.V., and Hajnal, Z., 2000, Crustal suture preserved in the Paleoproterozoic Trans-Hudson orogen, Canada: Geology, v. 28, p. 527–530, doi: 10.1130/0091-7613(2000)28<527:CSPITP>2.0.CO;2.

Wilde, S.A., Zhao, G.C., and Sun, M., 2002, Development of the North China Craton during the late Archean and its final amalgamation at 1.8 Ga; some speculations on its position within a global Paleoproterozoic supercontinent: Gondwana Research, v. 5, p. 85–94, doi: 10.1016/S1342-937X(05)70892-3.

Wu, F.Y., Zhao, G.C., Wilde, S.A., and Sun, D.Y., 2005, Nd isotopic constraints on the crustal formation of the North China Craton: Journal of Asian Earth Sciences, v. 24, p. 523–545, doi: 10.1016/j.jseaes.2003.10.011.

Zhai, M.G., Gao, J.H., and Liu, W.J., 2005, Neoarchean to Paleoproterozoic continental evolution and tectonic history of the North China Craton: A review: Journal of Asian Earth Sciences, v. 24, p. 547–561, doi: 10.1016/j.jseaes.2004.01.018.

Zhao, G.C., Wilde, S.A., Cawood, P.A., and Sun, M., 2001, Archaean blocks and their boundaries in the North China Craton: Lithological, geochemical, structural and P-T path constraints and tectonic evolution: Precambrian Research, v. 107, p. 45–73, doi: 10.1016/S0301-9268(00)00154-6.

Zhao, G.C., Sun, M., Wilde, S.A., and Li, S.Z., 2005, Late Archaean to Palaeoproterozoic evolution of the North China Craton: key issues revisited: Precambrian Research, v. 136, p. 177–202, doi: 10.1016/j.precamres.2004.10.002.

Zhao, L., Zheng, T.Y., and Lü, G., 2008, Insight into the craton evolution: Constraints from shear wave splitting in the North China Craton: Physics of the Earth and Planetary Interiors, v. 168, p. 153–162, doi: 10.1016/j.pepi.2008.06.003.

Zheng, T.Y., Chen, L., Zhao, L., Xu, W.W., and Zhu, R.X., 2006, Crust-mantle structure difference across the gravity gradient zone in North China Craton: Seismic image of the thinned continental crust: Physics of the Earth and Planetary Interiors, v. 159, p. 43–58, doi: 10.1016/j.pepi.2006.05.004.

Manuscript received 16 October 2008
Revised manuscript received 2 December 2008
Manuscript accepted 5 December 2008

Printed in USA